

RESEARCH ARTICLE

What are the optimum discrete angles to use in thermal-infrared radiative transfer calculations?

Robin J. Hogan^{1,2} ¹European Centre for Medium-Range
Weather Forecasts, Reading, UK²Department of Meteorology, University
of Reading, Reading, UK**Correspondence**Robin J. Hogan, ECMWF, Shinfield Park,
Reading, RG6 9AX, UK.Email: r.j.hogan@ecmwf.int**Abstract**

As computer power increases, there is a need to investigate the potential gains of using more than two streams in the radiative transfer calculations of weather and climate models. In this article, seven quadrature schemes for selecting the zenith angles and weights of these streams are evaluated rigorously in terms of the accuracy of thermal-infrared radiative transfer calculations. In addition, a new method is presented for generating “optimized” angles and weights that minimize the thermal-infrared irradiance and heating-rate errors for a set of clear-sky training profiles. It is found that the standard approach of applying Gauss–Legendre quadrature in each hemisphere is the least accurate of all those tested for two and four streams. For clear-sky irradiance calculations, “optimized” quadrature is between one and two orders of magnitude more accurate than Gauss–Legendre for any number of streams. For all-sky calculations in which scattering becomes important, a form of Gauss–Jacobi quadrature is found to be most accurate for between four and eight streams, but with Gauss–Legendre being the most accurate for 10 or more streams. No single quadrature scheme performs best in all situations, because computing irradiances involves two different integrals over angle and the relative importance of each integral depends on the amount of scattering taking place. Additional optimized quadratures for clear-sky and all-sky calculations with four to eight streams are presented that constrain the relationships between angles in a way that reduces the number of exponentials that need to be computed in a radiative transfer solver.

KEYWORDS

discrete ordinate method, heating rate, infrared radiative transfer, numerical convergence, two-stream approximation

1 | INTRODUCTION

The discrete ordinate method (Chandrasekhar, 1960) is widely used for 1D plane-parallel radiative transfer problems, and involves discretizing the diffuse radiation field into $2N$ zenith angles. The simplest two-stream ($N = 1$)

version was originally proposed by Schuster (1905), and over a century later the two-stream approach still underpins almost all weather and climate models worldwide. At the European Centre for Medium-Range Weather Forecasts (ECMWF), the radiation scheme accounts for only 3.5% of the computational cost of the 9-km resolution

model (Hogan & Bozzo, 2018), and this is likely to decrease with the planned upgrade of gas optical properties (Hogan & Matricardi, 2022). It is therefore important to investigate the additional accuracy, and possibly reduction in regional temperature biases, that could be obtained by increasing the number of streams from two to four or maybe more. In the thermal infrared (hereafter “longwave”), this could be facilitated by the finding of Fu et al. (1997) that, by approximating the treatment of scattering, the additional cost of the radiative transfer solver in moving from two to four streams can be reduced from a factor of 9.0 to a factor of 1.8.

This article is concerned with determining the optimal discrete angles to use for the modest number of streams that could be afforded in the longwave part of the radiation scheme in a weather or climate model. One might think that this matter would be settled: the undisputed standard for performing reference plane-parallel radiation calculations in the shortwave and longwave is the Discrete Ordinate Radiative Transfer package (DISORT: Stamnes et al., 1988), which only offers “double-Gauss” quadrature (Sykes, 1951), whereby the cosine of the zenith angle, μ , is discretized separately in each hemisphere using Gauss–Legendre quadrature. However, in the two-stream case this results in the single quadrature point $\mu_1 = 1/2$, corresponding to a discrete zenith angle of $\theta_1 = 60^\circ$. Despite having been used in two-stream schemes for thermal radiative transfer problems (e.g., Hogan, 2019; Schuster, 1905; Toon et al., 1989), it has been found (e.g., Rodgers & Walshaw, 1966) that much more accurate irradiances and heating rates are achieved using the Elsasser (1942) value of $\mu_1 = 1/1.66$, corresponding to $\theta_1 = 53^\circ$, and indeed this value is used in most weather and climate models worldwide. If Gauss–Legendre quadrature is suboptimal for two-stream longwave radiative transfer, it is legitimate to question its use for larger numbers of streams.

Li (2000) made an important contribution in his investigation of alternative longwave Gaussian quadrature schemes, and tested them with up to six streams using a single atmospheric profile in the absence of scattering. This is a springboard for the present study. In Section 2 we show how the two angular integrals in longwave radiative transfer (one to represent scattering and the other to convert the radiance distribution to an irradiance) lead to conflicting requirements on the “optimal” choice of quadrature angles. We give a physical explanation of why Li’s “Gaussian quadrature with different moment powers” leads to better performance than Gauss–Legendre.

An alternative to Gaussian quadrature was proposed by Lacis and Oinas (1991), who used three values per hemisphere of $\mu_1 = 0.1$, $\mu_2 = 0.5$, and $\mu_3 = 1$, with hand-tuned weights. In a no-scattering longwave solver, the transmittance of a layer of optical depth τ for stream i is

$T_i = \exp(-\tau/\mu_i)$. The computational advantage of using μ values that are multiples of each other is that the N exponentials may then be replaced by one exponential plus a few multiplications (in this case four: $T_{\text{tmp}} = T_1 \times T_1$, $T_2 = T_{\text{tmp}} \times T_{\text{tmp}} \times T_1$ and $T_3 = T_2 \times T_2$). This quadrature is still used in the no-scattering longwave solver of the NASA Goddard Institute for Space Studies (GISS) climate model.

In Section 3 we demonstrate a new method, in which angles and weights are chosen that formally minimize the mean-squared error in irradiances and heating rates for a set of 50 training profiles. A variant of this method is to constrain the μ values to be in a certain ratio, enabling the Lacis and Oinas (1991) optimization to be applied. In Section 4, seven quadrature schemes are evaluated on 50 independent clear-sky (i.e., no-scattering) evaluation profiles for up to 32 streams. Then in Section 5 a global model snapshot is used to evaluate the schemes in cloudy (scattering) situations, which involved modifying DISORT to use user-supplied quadrature angles. The conclusions in Section 6 provide recommendations for the appropriate quadrature depending on the number of streams and whether or not scattering is to be represented.

2 | THEORETICAL BASIS

2.1 | Scattering and irradiance integrals

The azimuthally averaged longwave radiative transfer equation for a plane-parallel (i.e., horizontally homogeneous) atmosphere may be written as (e.g., Fu et al., 1997)

$$\mu \frac{dI_\nu(\tau_\nu, \mu)}{d\tau_\nu} = I_\nu(\tau_\nu, \mu) - (1 - \omega_\nu)B_\nu - \frac{\omega_\nu}{2} \int_{-1}^1 p_\nu(\mu', \mu) I_\nu(\tau, \mu') d\mu', \quad (1)$$

where I_ν is the radiance at frequency ν , τ_ν is the optical depth of the atmosphere measured downwards from the top of the atmosphere (TOA) and acting as our vertical coordinate, μ is the cosine of the zenith angle of the beam and is positive for upward-propagating radiation and negative for downward, ω_ν is the single-scattering albedo of the medium, B_ν is the Planck function, and $p_\nu(\mu', \mu)$ is the azimuthally averaged scattering phase function representing the probability of light travelling in direction μ' being scattered into direction μ . Thus the three terms on the right-hand side represent respectively loss of radiation by extinction out of the beam, gain of radiation by emission into the beam, and gain of radiation by scattering into the beam. For the remainder of the article we drop the ν subscript for brevity.

The discrete ordinate method for approximating and efficiently solving Equation 1 involves discretizing the radiation field into $2N$ discrete directions μ_1 to μ_{2N} , such that

$$\mu_i \frac{dI(\tau, \mu_i)}{d\tau} = I(\tau, \mu_i) - (1 - \omega)B - \frac{\omega}{2} \sum_{j=1}^{2N} w'_j p(\mu_j, \mu_i) I(\tau, \mu_j), \quad (2)$$

where w'_j is the weight to be applied to direction μ_j in the numerical quadrature scheme. So how should we choose the optimum quadrature angles and weights? The scattering integral in Equation 1 is unweighted by μ' , suggesting that if the integrand can be approximated by a polynomial in μ' , Gauss–Legendre would be optimal. Indeed, Chandrasekhar (1960) proposed Gauss–Legendre quadrature across the full range $-1 \leq \mu' \leq 1$, which in the case of $N = 1$ results in quadrature angles of $\mu_{1,2} = \pm 3^{-1/2}$. One problem with this choice is that there is invariably a discontinuity in the radiance field at the horizon that is poorly sampled by Gauss–Legendre quadrature because it places angles more densely at the ends of the range than in the middle. This led Sykes (1951) to propose “double-Gauss” quadrature, whereby the two μ' ranges of -1 to 0 and 0 to 1 are discretized separately using Gauss–Legendre quadrature. This is the approach taken in DISORT (Stamnes et al., 1988).

It is important to recognise that the scattering integral in Equation 1 is not the only consideration when discretizing μ space, especially for longwave radiative transfer, where scattering tends not to be the dominant process, and in clear skies it is not important at all. In a weather or climate model we are concerned with irradiances, that is, the power passing through a horizontal plane at a particular height, which for upwelling irradiance may be written in continuous form as

$$F(\tau) = 2\pi \int_0^1 \mu I(\tau, \mu) d\mu, \quad (3)$$

and similarly for the downwelling irradiance. We see immediately that the integral weights the radiance by the cosine of the zenith angle μ ; indeed, this equation is a form of Lambert’s cosine law. The Sykes (1951) approach to discretizing Equation 3 is to use the same Gauss–Legendre angles and weights as previously, resulting in

$$F(\tau) \simeq 2\pi \sum_{j=1}^N w'_j \mu_j I(\tau, \mu_j), \quad (4)$$

where the indices $j = 1$ to N correspond to the upward-propagating radiances at different angles.

However, the Gauss–Legendre placement of μ values symmetrically in the 0 – 1 interval is not likely to be optimal for computing longwave irradiances; the weighting by μ in Equation 3 means that the optimal angles should be weighted more towards the zenith ($\mu = 1$) and nadir ($\mu = -1$) than the horizon ($\mu = 0$). This goes some way to explaining why, in the two-stream case, the Elsasser (1942) value of $\mu_1 = 1/1.66 = 0.602$ performs better than the Gauss–Legendre value of 0.5 (see Section 1).

Effectively, the Sykes (1951) approach treats Equation 3 as an unweighted integral of the function $\mu I(\tau, \mu)$. If we treat it as the integral of $I(\tau, \mu)$ weighted by μ , then this suggests we should use alternative quadratures designed for weighted integrals, leading to a discretization of the form

$$F(\tau) \simeq \pi \sum_{j=1}^N w_j I(\tau, \mu_j). \quad (5)$$

The angles μ_j must be the same as used for discretizing the scattering integral in Equation 2, even if calculated using an alternative method to Gauss–Legendre, but the weights are different, since w_j folds in the μ dependence, yet like w'_j must be normalized to satisfy

$$\sum_{j=1}^N w_j = 1. \quad (6)$$

From this point until the end of Section 4 we consider only clear-sky atmospheres in which Equation 3 is the only integral to be discretized; then in Section 5 we consider more realistic profiles containing clouds in which the scattering integral becomes important as well. At that point the relationship between the weights w'_j and w_j is provided.

2.2 | Optimizing transmittance

In order to establish a theoretical basis for alternative quadrature schemes optimized for longwave irradiance calculations, consider the transmittance of a slab of optical thickness τ illuminated from one side by isotropic radiation:

$$T(\tau) = 2 \int_0^1 \exp\left(-\frac{\tau}{\mu}\right) \mu d\mu, \quad (7)$$

which is the exponential integral of the third kind. The black solid line in Figure 1a depicts $T(\tau)$ computed numerically with extremely fine resolution in μ . In the absence of scattering and emission, the transmittance of a slab is equivalent to the ratio of irradiances at the far and near ends of the slab. Therefore, optimizing for transmittance is similar to optimizing for irradiances in the full

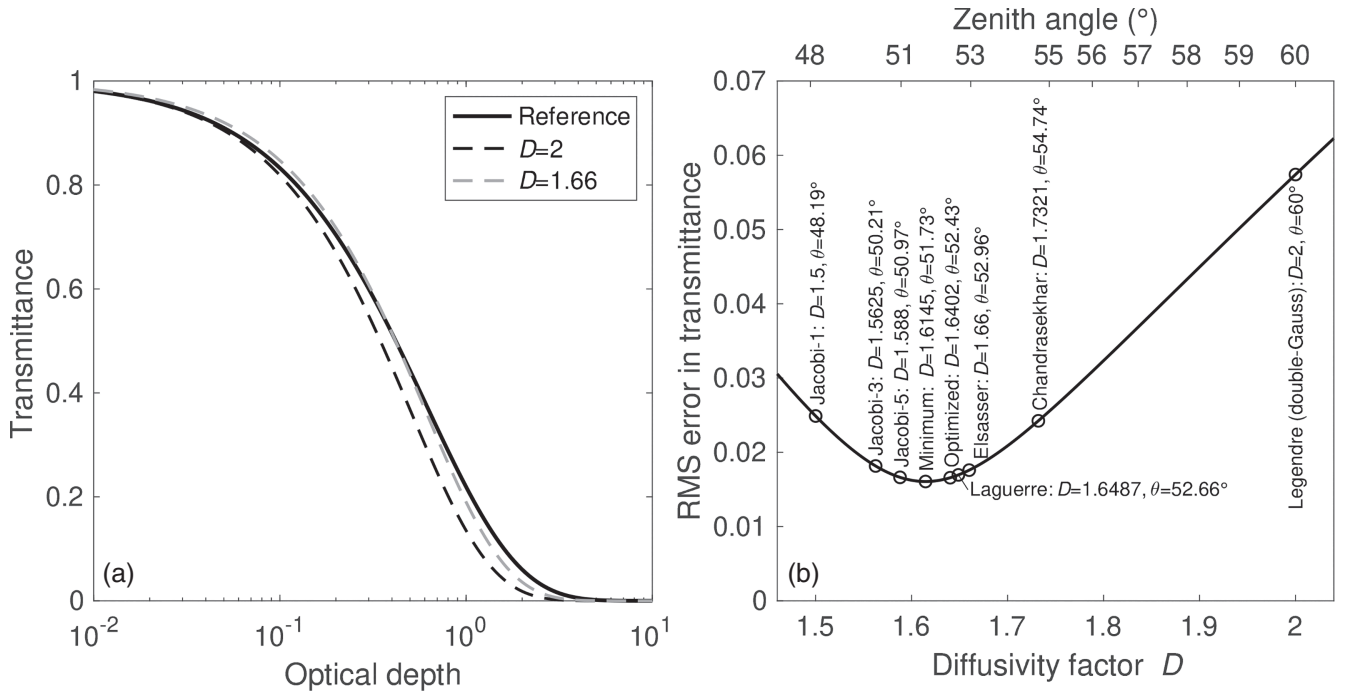


FIGURE 1 (a) Transmittance T of a slab of varying optical depth τ to isotropic radiation, and two approximations of the form $T = \exp(-D\tau)$. (b) Root-mean-squared error (RMSE) in transmittance versus D for this approximation, along with specific values of D discussed in the text (where “Legendre”, “Laguerre”, and “Jacobi” refer to Gauss–Legendre, Gauss–Laguerre, and Gauss–Jacobi quadrature) and the corresponding effective zenith angle is $\theta_1 = \cos^{-1}(1/D)$.

longwave radiative transfer problem. In the two-stream approximation, Equation 7 reduces to

$$T_{\text{TS}}(\tau, D) = \exp(-\tau/\mu_1) = \exp(-D\tau), \quad (8)$$

where all radiation is treated as propagating with zenith angle $\theta_1 = \cos^{-1}\mu_1$. This angle is usually expressed in terms of a diffusivity factor $D = 1/\mu_1$. In Figure 1a we see that the Gauss–Legendre value of $D = 2$ underestimates transmittance for all optical depths, although it is correct in the limit of very small optical depth. Elsasser’s value of 1.66 performs much better; indeed, he derived it simply by fitting these two curves by eye. Nonetheless, it does tend to overestimate transmittance at low optical depth and underestimate it at high optical depth.

We can be more systematic than Elsasser by computing the root-mean-squared error (RMSE) in transmittance for different values of D . To do this requires a distribution of optical depths to be specified. We do this by assuming a uniform distribution of transmittances, leading to the RMSE being given by

$$\text{RMSE}(D)^2 = \int_0^{\infty} [T_{\text{TS}}(\tau, D) - T(\tau)]^2 \frac{dT(\tau)}{d\tau} d\tau, \quad (9)$$

which is shown versus D [and equivalently $\theta_1 = \cos^{-1}(1/D)$] in Figure 1b. Also shown are values of D

associated with specific schemes discussed in this article. We see that the Gauss–Legendre value of $D = 2$ is very far from optimal: the minimum error in fact occurs for $D = 1.6145$, although Elsasser’s value is close to the minimum. As will be demonstrated in later sections of this article, there is no single “correct” value for D , because one value does not perfectly reproduce the transmittance for all optical depths in Figure 1a, and the optical depth of the atmosphere varies strongly with wavelength and absorber amount. Even at a single wavelength, the spectral heating rate at a particular altitude depends on the transmittance to all other layers as well as to the surface and TOA. This has not prevented proposals for parametrizing D as a function of optical depth (DeSouza-Machado et al., 2020; Zhao & Shi, 2013) or using a different value for different parts of the spectrum (Feng & Huang, 2019).

2.3 | Gaussian quadrature schemes

Finally, in this section we present the theoretical basis for alternative Gaussian quadrature schemes for longwave radiative transfer. While the schemes proposed are similar to those examined by Li (2000), some important additional insights are presented on why they should work better than Gauss–Legendre quadrature. An introduction to alternative Gaussian quadrature schemes

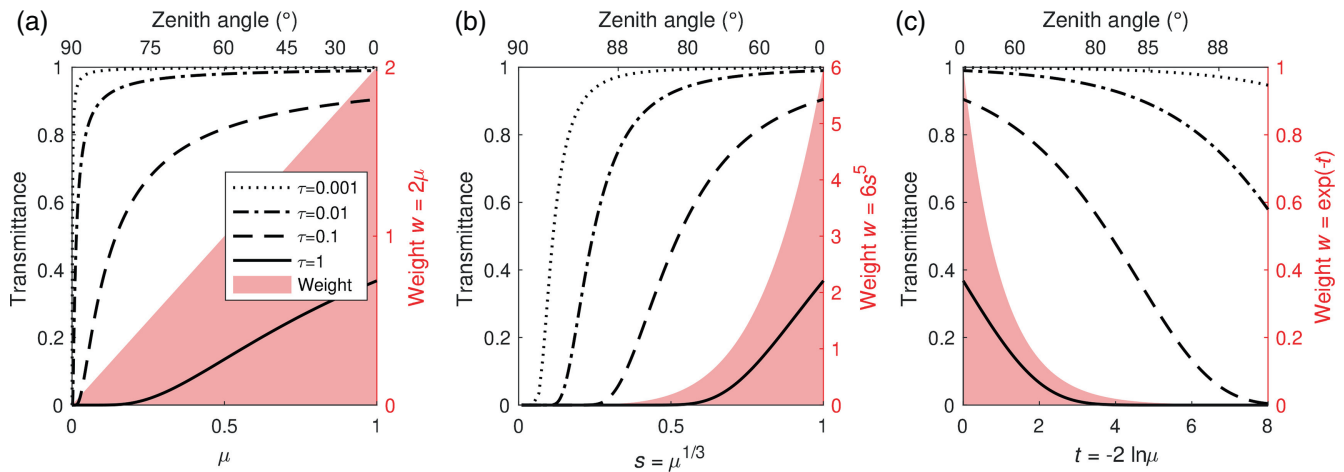


FIGURE 2 (a) Transmittance T of a slab of optical depth τ to a beam propagating with a zenith-angle cosine of μ ; the shading [red in the online version] indicates the weighting when integrating over μ to compute the transmittance to isotropic incident radiation (see Equation 7). (b) The same but after a change of variables $s = \mu^{1/3}$ to make the transmittance $T(s)$ more amenable to numerical quadrature; the resulting weighting by $w = 6s^5$ leads to the Gauss–Jacobi-5 quadrature rule. (c) As (a) but with an alternative change of variables, the exponential weight function of which leads to the Gauss–Laguerre quadrature rule.

is provided by Press et al. (2007); the corresponding nodes and weights can be derived from the values in tables 25.8 and 25.9 of Abramowicz and Stegun (1972), although we compute them using a free-software package implementing the algorithm described by Kautsky and Elhay (1982).

The choice of Gaussian quadrature scheme depends firstly on the functional form of the weight term, which in Equations 5 and 7 is simply $w(\mu) = 2\mu$ for integration in the interval $0 \leq \mu \leq 1$ and is illustrated by the shaded area in Figure 2a. Gauss–Jacobi quadrature deals with weights of general form $w(x) = (1-x)^\alpha(1+x)^\beta$ for integration in the interval $-1 \leq x \leq 1$, so is appropriate for our problem with the substitutions $\mu = (x+1)/2$, $\alpha = 0$, and $\beta = 1$. For the two-stream problem (i.e., a single angle in the μ interval from 0 to 1), this quadrature proposes $\mu_1 = 2/3$. This is shown as “Jacobi 1” (because $\beta = 1$) in Figure 1b where, despite being better than unweighted Gauss–Legendre quadrature, it is still clearly not the best choice, and indeed for more than two streams the same is found when applied to real atmospheric profiles. The problem is that, to be well approximated by a Gaussian quadrature rule, the integrand should be well approximated by a polynomial, with N -point Gaussian quadrature being exact for polynomials up to degree $2N - 1$. Figure 2a shows the transmittance of a single beam of radiation, that is, the function $\exp(-\tau/\mu)$, for four different optical depths, and it would clearly not be well fitted by a low-order polynomial, especially at low optical depths.

The situation is improved with a change of variables. For example, if we use a variable of integration $s = \mu^{1/\gamma}$

then Equation 7 becomes

$$T(\tau) = 2\gamma \int_0^1 s^{2\gamma-1} \exp\left(-\frac{\tau}{s^\gamma}\right) ds. \quad (10)$$

Figure 2b shows that the integrand $\exp(-\tau/s^\gamma)$, here for the case of $\gamma = 3$, varies somewhat more smoothly with s and therefore we should expect the quadrature scheme to be more accurate. The weight function now has the form $w(s) = 2\gamma s^{2\gamma-1}$, which integrates to unity in the s interval 0–1 and is shown by the shaded area in Figure 2b. Gauss–Jacobi quadrature may still be used but with $\beta = 2\gamma - 1$, leading to the weight function taking the form $w(s) = (\beta + 1)s^\beta$. Table 25.8 of Abramowicz and Stegun (1972) provides the nodes and weights for β up to 5 and N up to 8, or an off-the-shelf software package for computing Gauss–Jacobi quadrature can be used for any value of β and N . The resulting set of nodes s_1 to s_N needs to be transformed back to μ -space with $\mu_i = s_i^\gamma$. Figure 1b shows the two-stream performance of Gauss–Jacobi quadrature for a change of variables with $\gamma = 2$ (“Jacobi 3”) and $\gamma = 3$ (“Jacobi 5”), both of which are significantly nearer the minimum in the error curve. Li (2000) also explored the use of various Gauss–Jacobi quadrature schemes, although what we refer to as “Gauss–Jacobi- β ” quadrature he referred to as “Gaussian quadrature with moment power β ” (but note that he used the symbol m in place of β). Li (2000) did not explain why values of β larger than 1 should perform better, so hopefully the explanation here in terms of a change of variables resulting in the integrand being closer to a polynomial, for which Gaussian quadrature is designed, is valuable.

An alternative change of variables involves the use of a logarithmic scale for μ , that is, $t = -2 \ln \mu$, resulting in Equation 7 becoming

$$T(\tau) = \int_0^\infty \exp(-t) \exp\left[-\frac{\tau}{\mu(t)}\right] dt. \quad (11)$$

It is apparent from Figure 2c that this makes the integrands even better behaved, although it does increase the domain of integration from 0–1 to 0– ∞ , which will be shown later in the article to be a disadvantage for large orders of quadrature N . The appropriate quadrature scheme for a weight function of $w(t) = \exp(-t)$ is Gauss–Laguerre, the nodes of which need to be transformed back to μ -space with $\mu_i = \exp(-t_i/2)$. For $N = 1$, Gauss–Laguerre produces $D = 1/\mu_1 = 1.6487 = e^{1/2}$, which can be seen in Figure 1b to be very close to the Elsasser value but a little closer to the minimum of the error curve.

Table 1 presents the angles and weights of the Gauss–Laguerre and Gauss–Jacobi-5 quadratures for N up to 4. We show Gauss–Jacobi only in the $\beta = 5$ case, because in Section 4 it is found to be superior to all other values of β .

Li (2000) extended Gauss–Jacobi quadrature up to a moment power of $\beta = \infty$, in which limit off-the-shelf numerical schemes for computing nodes and weights no longer work. Nonetheless, he was able to compute the nodes and weights analytically up to $N = 3$. Intriguingly, his values (see his equations A7, A9, and A13) exactly match those computed from Gauss–Laguerre quadrature, so we conclude that the latter is equivalent to Gauss–Jacobi quadrature with $\beta = \infty$ and the appropriate changes of variables. It is beyond the scope of this article to prove this equivalence mathematically, but it is convenient for those who might want to try the $\beta = \infty$ quadrature proposed by Li (2000) for $N > 3$ to know that it can be

TABLE 1 The cosine-angles μ and weights w for five quadrature schemes: Gauss–Laguerre, Gauss–Jacobi with $\beta = 5$, and three “optimized” schemes, where the number of angles per hemisphere N ranges from 1–4.

N	Variable	Gauss–Laguerre	Gauss–Jacobi-5	Optimized	Optimized-IR	Optimized-IRJP
1	μ	0.6065306597	0.6297376093	0.6096748751		
	w	1.0000000000	1.0000000000	1.0000000000		
2	μ	0.1813898346	0.2509907356	0.1976969570	0.1828926897	0.2669139064
		0.7461018061	0.7908473988	0.7419416274	0.7315707589 (×4)	0.8007417192 (×3)
	w	0.1464466094	0.2300253764	0.1520985621	0.1352478522	0.2509036055
3	μ	0.8535533906	0.7699746236	0.8479014379	0.8647521478	0.7490963945
		0.0430681066	0.1024922169	0.0661385934	0.0675169363	0.1073702810
		0.3175435896	0.4417960320	0.3440369508	0.3375846814 (×5)	0.4294811240 (×4)
	w	0.8122985952	0.8633751621	0.8156973793	0.8102032354 (×12)	0.8589622480 (×8)
		0.0103892565	0.0437820218	0.0197413567	0.0197437659	0.0445786516
		0.2785177336	0.3875796738	0.2857816420	0.2746853796	0.3679447208
4	μ	0.7110930099	0.5686383044	0.6944770013	0.7055708545	0.5874766276
		0.0091177205	0.0454586727	0.0259142819	0.0263733596	0.0468366244
		0.1034869099	0.2322334416	0.1420093170	0.1318667980 (×5)	0.2341831222 (×5)
		0.4177464746	0.5740198775	0.4312455503	0.4219737537 (×16)	0.6088761177 (×13)
	w	0.8510589811	0.9030775973	0.8441789463	0.8439475074 (×32)	0.9367324887 (×20)
		0.0005392947	0.0092068785	0.0030584329	0.0028332575	0.0093955477
		0.0388879085	0.1285704278	0.0539378694	0.0476214091	0.1353113093
		0.3574186924	0.4323381850	0.3332755640	0.3349230090	0.5081423593
		0.6031541043	0.4298845087	0.6097281337	0.6146223244	0.3471507838

Note: The suffix “IR” indicates that a prescribed “integer ratio” applies between each μ value and the first (indicated in brackets), enabling the number of exponentials in downstream calculations to be reduced. The suffix “JP” indicates that an additional “Jacobi prior” has been added to the cost function, penalizing the difference between optimized μ and w values and their Gauss–Jacobi-5 equivalents, making Optimized-IRJP well suited for scattering atmospheres.

computed easily using an off-the-shelf Gauss–Laguerre algorithm, or taken from table 12.9 of Abramowitz and Stegun (1972).

Li (2000) argued that the most accurate quadrature schemes for longwave radiative transfer arise from using the highest moment power, that is, the largest value of β ; the logic of this paragraph would suggest that this is Gauss–Laguerre quadrature. This was partially based on how close its two-stream diffusivity was to Elsasser’s value of 1.66, although since the latter was fitted to the transmittance curve by eye we would argue that there is nothing particularly special about it, and we can see from Figure 1b that, in terms of transmittance at least, values of D in the range 1.57–1.66 are at least as accurate as Elsasser’s value and there is little to choose between them. Ultimately, the test of a quadrature scheme should be in its performance on real atmospheric profiles in both clear-sky and cloudy conditions, and this is pursued rigorously in Sections 4 and 5.

3 | OPTIMIZED QUADRATURE FOR CLEAR-SKY RADIATIVE TRANSFER

Figure 1b demonstrated that, in the $N = 1$ case, Gaussian quadrature is not the only basis on which to select angles and weights: we can instead seek the value or values that minimize some scalar measure of overall error with respect to a reference calculation. In this section we extend this idea to more than one angle and use real atmospheric profiles. Hogan and Matricardi (2022) showed that the gas-optics part of a radiative transfer scheme could be improved significantly by optimizing the absorption coefficients of the look-up tables in order to improve the agreement with line-by-line calculations for a set of reference profiles. Here we take a similar approach but optimize the angles and weights of a quadrature scheme. We use the 50 present-day profiles of the “Evaluation-1” dataset from the Correlated K-Distribution Model Intercomparison Project (CKD-MIP; Hogan and Matricardi 2020), which are defined on 54 atmospheric layers that extend up to a pressure of 0.01 hPa and cover a wide range of temperature, humidity, and ozone concentrations. The well-mixed gases are N_2 , O_2 , CO_2 , CH_4 , N_2O , CFC-11, and CFC-12, and neither clouds nor aerosols are represented. The gas-optics model used is “FSC-32” described by Hogan and Matricardi (2022), which divides the entire longwave spectrum into 32 noncontiguous spectral intervals. Here and throughout this article we neglect the effects of Earth curvature.

Following Hogan and Matricardi (2022), we minimize a cost function of the form

$$J = \sum_{k=1}^n \left\{ \sum_{j=1}^m h_j \left(H_j^{\text{quad}} - H_j^{\text{ref}} \right)^2 + f \left[\left(F_{\uparrow\text{TOA}}^{\text{quad}} - F_{\uparrow\text{TOA}}^{\text{ref}} \right)^2 + \left(F_{\downarrow\text{surf}}^{\text{quad}} - F_{\downarrow\text{surf}}^{\text{ref}} \right)^2 \right] \right\}, \quad (12)$$

where the outer summation is over the n profiles, the inner summation is over the m layers, H_j denotes the heating rate of layer j in $K \cdot d^{-1}$, $F_{\uparrow\text{TOA}}$ denotes upwelling irradiance at TOA in $W \cdot m^{-2}$, $F_{\downarrow\text{surf}}$ denotes downwelling irradiance at the surface, the superscript “quad” represents values computed using the quadrature scheme, and the superscript “ref” represents reference values. Following Hogan (2010), we define the layer weights as proportional to the difference in the square-root of pressure across them, such that the contribution of the troposphere and stratosphere is approximately equal: $h_j = (p_{j+1/2}^{1/2} - p_{j-1/2}^{1/2}) / p_{m+1/2}^{1/2}$, where $p_{j+1/2}$ is the pressure of the interface between layers j and $j + 1$ (increasing from TOA towards the surface) and $p_{m+1/2}$ is the surface pressure. The user-specified value f balances the irradiance and heating-rate errors, and we have found that $f = 0.02 (K \cdot d^{-1})^2 / (W \cdot m^{-2})^2$ provides a satisfactory balance between the two in resulting radiative transfer calculations.

Since scattering can be neglected, the radiative transfer consists of projecting N beams of radiation up and down through the atmosphere, and for simplicity we set the surface emissivity to unity. Thus the initial radiance of each upward-propagating beam at the surface is equal to the Planck function at the surface, $B_{m+1/2}$, while the initial radiance of each downward-propagating beam at TOA is zero. Assuming the Planck function varies linearly with optical depth across a layer, the solution to Equation 2 for the downwelling radiance at angle μ_i at the base of layer j is (e.g., Clough et al., 1992)

$$I_{i,j+1/2} = I_{i,j-1/2} \exp\left(-\frac{\tau_j}{\mu_i}\right) + \left[1 - \exp\left(-\frac{\tau_j}{\mu_i}\right) \right] \left(B_{j-1/2} - \frac{\mu_i \Delta B_j}{\tau_j} \right) + \Delta B_j, \quad (13)$$

where τ_j is the zenith optical depth of the layer and $\Delta B_j = B_{j+1/2} - B_{j-1/2}$ is the difference in Planck function across the layer. This may be applied recursively from TOA down to the surface, and similarly for the upward-propagating beams. The irradiances may then be computed by applying Equation 5 to the radiances at the interface between each

layer. The reference calculations are performed with many hundreds of evenly spaced angles.

We define the “state vector”, \mathbf{x} , containing variables to be optimized as the N angles μ_1 to μ_N and all but one of the corresponding “normalized” weights W_1 to W_{N-1} , where $W_i = w_i/2\mu_i$. The use of normalized weights in the minimization makes each element of the state vector more similar in magnitude. The final normalized weight is computed from the others to ensure that Equation 6 holds:

$$W_N = \frac{1}{\mu_N} \left(1 - \sum_{j=1}^{N-1} W_j \mu_j \right). \quad (14)$$

The initial values of the state vector are such that the angles are evenly spread in μ -space and have equal normalized weight. The cost function is minimized by coding the radiative transfer (primarily Equation 13) in C++, and using the automatic differentiation and optimization library “Adept” (Hogan, 2014) to compute the gradient of the cost function with respect to all elements of the state vector, $\partial J/\partial \mathbf{x}$. The “L-BFGS” minimization algorithm of Liu and Nocedal (1989) calls the radiative transfer repeatedly with different values for \mathbf{x} , using $\partial J/\partial \mathbf{x}$ to find the \mathbf{x} that minimizes J .¹ The resulting “optimized” angles and weights are shown in Table 1 for N up to 4, and are evaluated against the Gaussian quadrature schemes using real atmospheric profiles in the next section.

Lacis and Oinas (1991) proposed an $N = 3$ quadrature in which the second and third μ values were multiples of the first, which meant that three exponentials could be replaced by one, thereby substantially speeding up radiative transfer calculations, the computational cost of which is often dominated by the exponential function. We implement this idea by choosing the integer ratios closest to those between the μ values emerging from the “optimized” quadrature in Table 1, and then repeating the optimization but retrieving only the smallest μ value and computing the others by applying these integer ratios. The resulting quadrature schemes up to $N = 4$ are shown in the penultimate “Optimized-IR” column of Table 1.

We may also find the closest integer-ratio quadrature scheme to an existing Gaussian scheme by adding a term to the cost function of the form

$$J_p = f_p \left[\sum_{j=1}^N (\mu_j - \mu_j^p)^2 + \left(W_j - W_j^p \right)^2 \right], \quad (15)$$

where μ_j^p and W_j^p are the “prior” nodes and normalized weights of an existing Gaussian quadrature scheme, and

f_p is the weight applied to the term. We find that a value of 0.001 provides the most accurate scheme. The final column of Table 1 shows the resulting “optimized-IRJP” quadrature scheme obtained using the Gauss–Jacobi-5 scheme as a prior. The motivation to remain close to Gauss–Jacobi-5 is that this scheme is found to be most accurate when scattering is introduced in Section 5.

4 | CLEAR-SKY EVALUATION OF QUADRATURE SCHEMES

In this section we evaluate various quadrature schemes in terms of their ability to predict clear-sky irradiances and heating rates. We use the 50 present-day profiles of the “Evaluation-2” dataset from CKDMIP (Hogan & Matricardi, 2020), which comprise a different set of profiles from the Evaluation-1 dataset used in Section 3. Again we use the “FSCK-32” gas-optics model described by Hogan and Matricardi (2022), and the same clear-sky radiative transfer algorithm.

Figure 3a depicts the RMSE in surface downwelling and TOA upwelling irradiance versus the number of streams from 2 to 32, for seven different quadrature schemes. The least accurate is Gauss–Legendre quadrature, also known as double-Gauss (Sykes, 1951), followed by Gauss–Laguerre, which is typically 5–8 times more accurate for a given number of streams. Both exhibit approximately fourth-order convergence, that is, when the number of streams is increased by a factor of f , RMSE reduces by around a factor of f^4 .

As explained in Section 2, Gauss–Jacobi quadratures may be constructed via a change of variables $s = \mu^{1/\gamma}$, resulting in the integration being weighted by s^β where $\beta = 2\gamma - 1$. We have tested a range of integer values of γ , and while the performance of values of 2, 3, and 4 is quite similar, we find that $\gamma = 3$ (i.e., $\beta = 5$) is superior, and this is shown as “Gauss–Jacobi-5” in Figure 3a and the remaining plots in this article. This quadrature scheme is superior to Gauss–Laguerre for all numbers of streams except 2; for 32 streams it is more than 40 times more accurate than Gauss–Laguerre and 400 times more accurate than Gauss–Legendre. Recall that Gauss–Laguerre quadrature is the same as Gauss–Jacobi in the limit of $\gamma \rightarrow \infty$. The “optimized” quadrature scheme generated using the method described in Section 3 performs a little better than Gauss–Jacobi-5 up to 24 streams, while the “optimized-IR” scheme (enforcing integer ratios between the retrieved μ values) for N between 2 and 4 performs only very slightly worse.

The reason that Gauss–Laguerre performs worse than the Gauss–Jacobi-5 and optimized quadratures for larger numbers of streams can be explained by the change of

¹The software is freely available at <https://github.com/rjhogan/optimize-angles>.

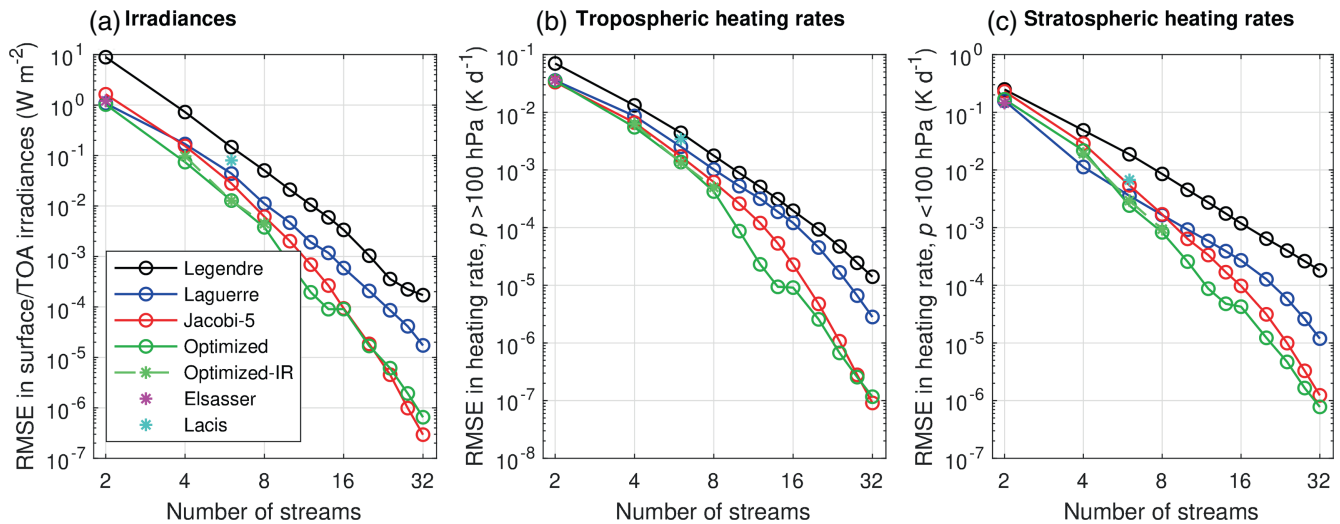


FIGURE 3 Root-mean-squared error (RMSE) in clear-sky (a) surface downwelling and TOA upwelling longwave irradiances, (b) heating rate for pressure, p , greater than 100 hPa, and (c) heating rate for p less than 100 hPa, for the 50 CKDMIP “Evaluation-2” profiles, as a function of the number of angular streams (equal to $2N$) using seven different quadrature schemes. The reference calculations use Gauss–Jacobi-5 quadrature (with 64 streams), since this is the most accurate of the Gaussian schemes.

variables of $t = -2 \ln \mu$ described in Section 2, which transforms an integral in the range 0–1 to one in the range 0– ∞ . For large N , Gauss–Laguerre quadrature places many quadrature points at large values of t but with vanishingly small weights. In angular space this wastes quadrature points on zenith angles very close to 90° , so the performance of the scheme in terms of RMSE is as if it had fewer quadrature points overall. This can already be seen for $N = 4$ in Table 1: Gauss–Laguerre has a node with a zenith angle of 89.5° but only 0.05% of the energy.

Figure 3a also shows the performance of Elsasser’s value for $N = 1$, and the Lacis and Oinas (1991) coefficients for $N = 3$ ($\mu_1 = 0.1$, $\mu_2 = 0.5$, $\mu_3 = 1$, $w_1 = 0.0432$, $w_2 = 0.5742$, and $w_3 = 0.3826$). The latter is better than Gauss–Legendre but worse than all the other quadrature schemes.

We next evaluate the heating rates computed by the various quadrature schemes. Figure 3b,c depicts the RMSE in tropospheric and stratospheric/mesospheric heating rates, respectively, according to whether the pressure is greater than or less than 100 hPa. In each case we follow Section 3 and weight each layer by the difference in the square root of pressure between the bottom and top of the layer. This time, the order of convergence of Gauss–Legendre quadrature with increasing N is closer to 2.8. Again, Gauss–Laguerre is more accurate than Gauss–Legendre, with Gauss–Jacobi-5 and then the optimized quadrature even more accurate, especially for larger numbers of streams. The exception is for stratospheric/mesospheric heating rates, where for four streams we find that Gauss–Laguerre is clearly the most accurate.

This again highlights that one set of quadrature points is not necessarily optimum for both irradiances and heating rates.

Figure 4 reveals that stratospheric/mesospheric heating-rate errors are largely associated with biases centred on the stratopause at around 1 hPa, and scale with the shape of the CO_2 -dominated cooling-rate profile (e.g., fig. 5 of Hogan & Matricardi, 2022). Gauss–Legendre quadrature overpredicts the cooling rate in all cases (negative heating-rate bias), while Gauss–Jacobi-5 tends to underpredict the cooling but with an amplitude somewhat smaller. For the two-stream ($N = 1$) case, very similar performance is found for Gauss–Laguerre, optimized quadrature, and Elsasser’s $D = 1.66$. This is because, as shown in Figure 1b, these schemes all have very similar values of D . For four streams ($N = 2$), Gauss–Laguerre quadrature is clearly the best, with virtually no bias in stratospheric heating rates, followed by optimized and optimized-IR. For six streams, these three schemes perform similarly well.

5 | ALL-SKY EVALUATION OF QUADRATURE SCHEMES

In this section we extend the evaluation to cloudy skies in which scattering becomes important. A modified version of the offline ecRad radiation scheme (Hogan & Bozzo, 2018) has been used in which DISORT (Stamnes et al., 1988) has been embedded as a solver. This way we take advantage of ecRad’s treatment of the optical

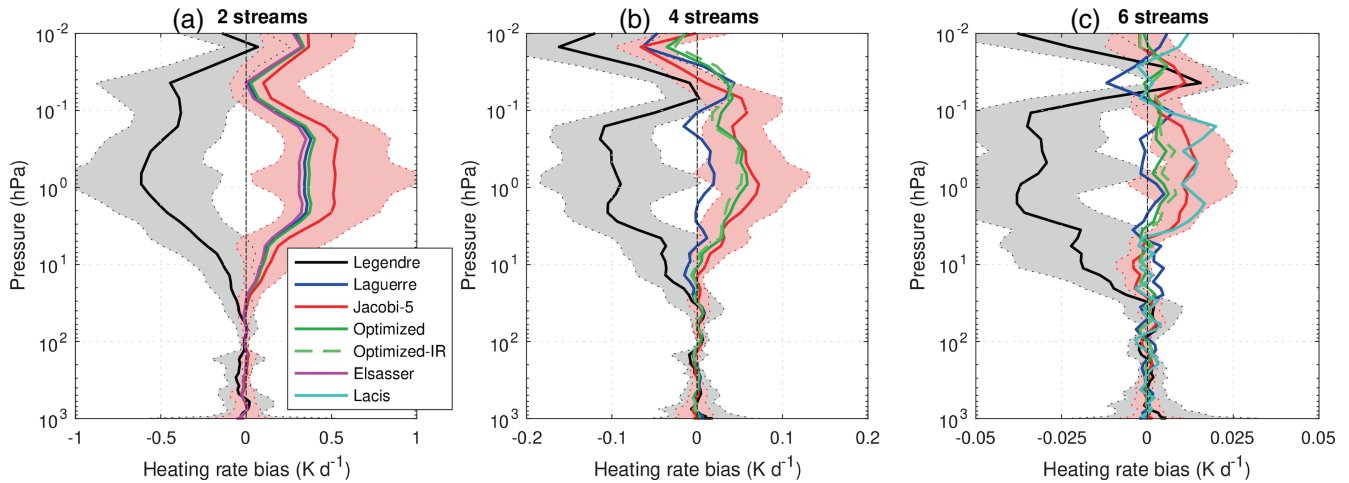


FIGURE 4 Solid lines: atmospheric heating rate biases for various quadrature schemes with (a) 2, (b) 4, and (c) 6 angular streams, using the 50 CKDMIP “Evaluation-2” clear-sky profiles. The shaded areas for Gauss–Legendre and Gauss–Jacobi-5 quadrature encompass 95% of the profiles (estimated as 1.96 times the standard deviation). Note that Elsasser is only for two streams, Lacis only for six streams and optimized-IR only for 4–6 streams.

properties of gases and clouds, and again use the fast FSCK-32 longwave gas-optics scheme. We have confirmed that the results presented in this section are insensitive to the gas-optics scheme used, having performed sensitivity tests (not shown) with the slower Rapid Radiative Transfer Model for Global Circulation Models (RRTMG: Mlawer et al. (1997) scheme also available in ecRad. We use Mie theory to generate phase functions for liquid droplets and the Baum et al. (2014) “general habit mixture” phase functions for ice particles. We run this ecRad-DISORT model on a 3D global snapshot of the latest ECMWF reanalysis (ERA5) at 1200 UTC on July 11, 2019 with 137 vertical levels and 1° resolution. Meyer et al. (2022) extracted a 2D slice from this exact scene to demonstrate features of ecRad, although here we neglect aerosols. Since DISORT cannot handle horizontal subgrid cloud heterogeneity, we compute the total cloud cover assuming the same exponential-random overlap as in the operational ECMWF model, and assume clouds fill the cloudy fraction of each column homogeneously. The gridbox-mean irradiances are then computed as the weighted average of a clear-sky and a cloudy column. While this would not be suitable for an operational radiation scheme because it neglects subgrid heterogeneity of cloud optical depth, it is adequate for estimating the relative accuracy of different quadrature schemes in all-sky conditions.

DISORT solves the coupled differential equations represented by Equation 2, now with the summation term representing scattering processes that was neglected in Section 4. DISORT has been modified so that the angles and weights may be configured by the user, rather than always being computed using Gauss–Legendre

quadrature. The weights w'_j in Equation 2 and w_j in Equation 5 both satisfy the normalization given by Equation 6. In the case of Gauss–Legendre quadrature, the symmetry in the placement of μ values in the interval 0–1 means that we can simply equate Equations 4 and 5 to obtain $w'_j = w_j/(2\mu_j)$, which is assumed implicitly by the DISORT code. For the other quadratures considered here, we have made a modification to DISORT so that the weights used in the scattering summation in Equation 2 satisfy

$$w'_j = \frac{w_j/\mu_j}{\sum_{i=1}^N w_i/\mu_i}. \quad (16)$$

While it may seem unsatisfactory that a different scaling is required for the quadrature weights when used to approximate two different integrals, it is simply a consequence of one of the integrals being weighted by μ and the other not. The fact that quadratures symmetric in the range 0–1 (such as Gauss–Legendre) can use the same set of weights for both integrals by applying Equation 4 instead of Equation 5 is not a strong argument for them, since energy can be conserved without this symmetry. Indeed, the widespread use of Elsasser’s value demonstrates this in the two-stream case. Fu et al. (1997) stated that the two-stream relationship between irradiance and radiance is $F = 2\pi\mu_1 I_1(\mu_1)$, but that for choices of μ_1 other than $1/2$ this should be replaced by $F = \pi I_1(\mu_1)$. Essentially the replacement of Equation 4 with Equation 5 is the $2N$ -stream generalization of the Fu et al. statement.

Figure 5 depicts the RMSE in irradiances and heating rates for the ERA5 scene, but this time for all-sky

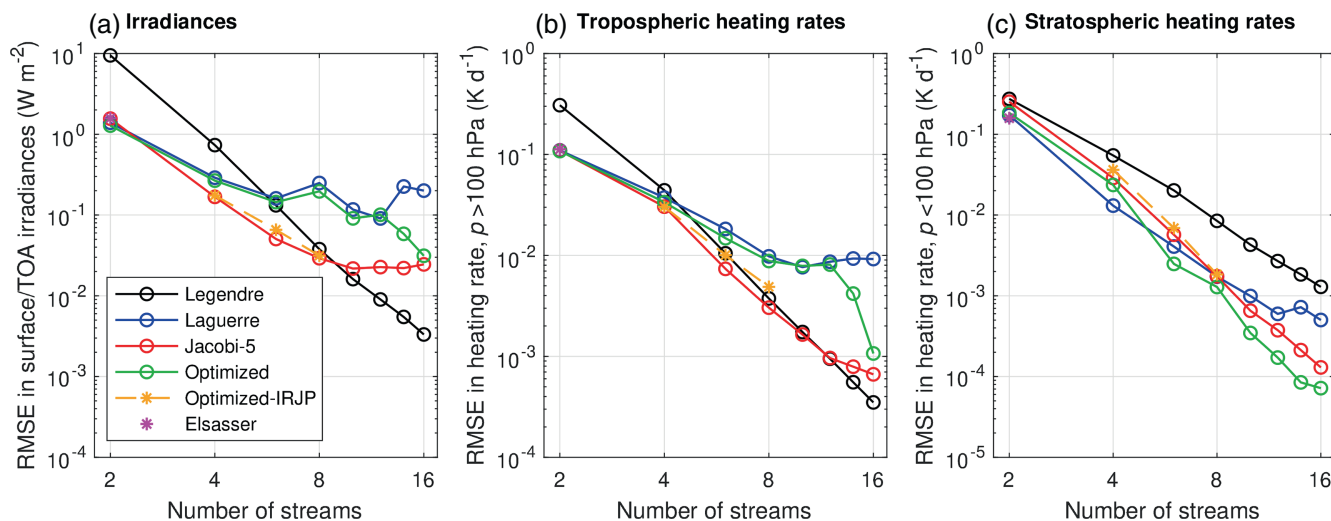


FIGURE 5 As Figure 3, but computed using ERA5 fields at 1200 UTC on July 11, 2019, for all-sky conditions with atmospheric scattering. The reference calculations use the most accurate Gaussian scheme with 32 streams: in (a) and (b) this is Gauss–Legendre quadrature and in (c) it is Gauss–Jacobi-5 quadrature.

conditions with scattering. The results for irradiances and tropospheric heating rates are very different from the clear-sky results in Figure 3a,b. As before, the Gauss–Laguerre, Gauss–Jacobi-5, and optimized quadrature schemes all outperform Gauss–Legendre with two and four streams, but for larger N they tend to approach an asymptotic RMSE regardless of N . By contrast, Gauss–Legendre quadrature continues to converge with N at much the same rate as for clear skies, and is the most accurate all-sky scheme for 16 streams. Gauss–Jacobi-5 is clearly better than Gauss–Laguerre and optimized quadrature, still outperforming Gauss–Legendre quadrature up to and including the eight-stream case. Optimized-IRJP quadrature is intended to provide the closest quadrature to Gauss–Jacobi-5 but with μ values in fixed integer ratios, and indeed it is only a little less accurate than Gauss–Jacobi-5. The heating-rate errors in the cloud-free stratosphere/mesosphere are, by contrast, virtually identical between Figures 3c and 5c.

The explanation for the all-sky behaviour in Figure 5a,b is as follows. The optimum quadrature schemes for the scattering integral in Equation 1 and the irradiance integral in Equation 3 are clearly different, due to only one being weighted by μ . In the longwave, gaseous absorption and emission are fundamental, while scattering is of secondary importance. This means that errors in calculations of irradiances and heating rates using a small number of streams are dominated by errors in vertical transmission. Using a quadrature scheme optimized for the transmission problem means that errors reduce rapidly with increasing N , until errors due to scattering begin to dominate, for which such a quadrature scheme is less well

suited. One might expect convergence to continue, albeit at a slower rate, but this is not observed in Figure 5a. The reason is believed to be the fact that the phase function of clouds has a strong peak in the forward direction that cannot be resolved by discrete-ordinate radiative transfer calculations unless they have a much larger number of streams than considered here. DISORT addresses this with “delta- M ” scaling of the phase function (Wiscombe, 1977): the number of streams is used to determine what scale of angular structures in the phase function can be resolved adequately, and the part of the forward-scattering peak that cannot be resolved is treated as if it was not scattered at all. This works well for Gauss–Legendre quadrature, because its more even spacing of quadrature points in μ -space ensures that the part of the forward-scattering peak deemed to be ‘resolvable’ by the delta- M method is indeed adequately resolved. This is less the case for the other quadrature schemes. It is beyond the scope of this article to see whether modifying the delta- M method would be advantageous for other quadrature schemes.

We stress that the primary purpose of this article is to explore the appropriate quadrature scheme to use in weather and climate models if four or even six streams could be afforded, and it is clear from Figure 5a that Gauss–Jacobi-5 incurs longwave irradiance errors around four times less than Gauss–Legendre, even when clouds are present. However, for using DISORT to perform reference calculations, for which 128 streams is common, Gauss–Legendre quadrature should still be used.

Finally, we investigate the spatial pattern of irradiance errors and their dependence on column water vapour, for various quadrature schemes. Figures 6 and 7 show the

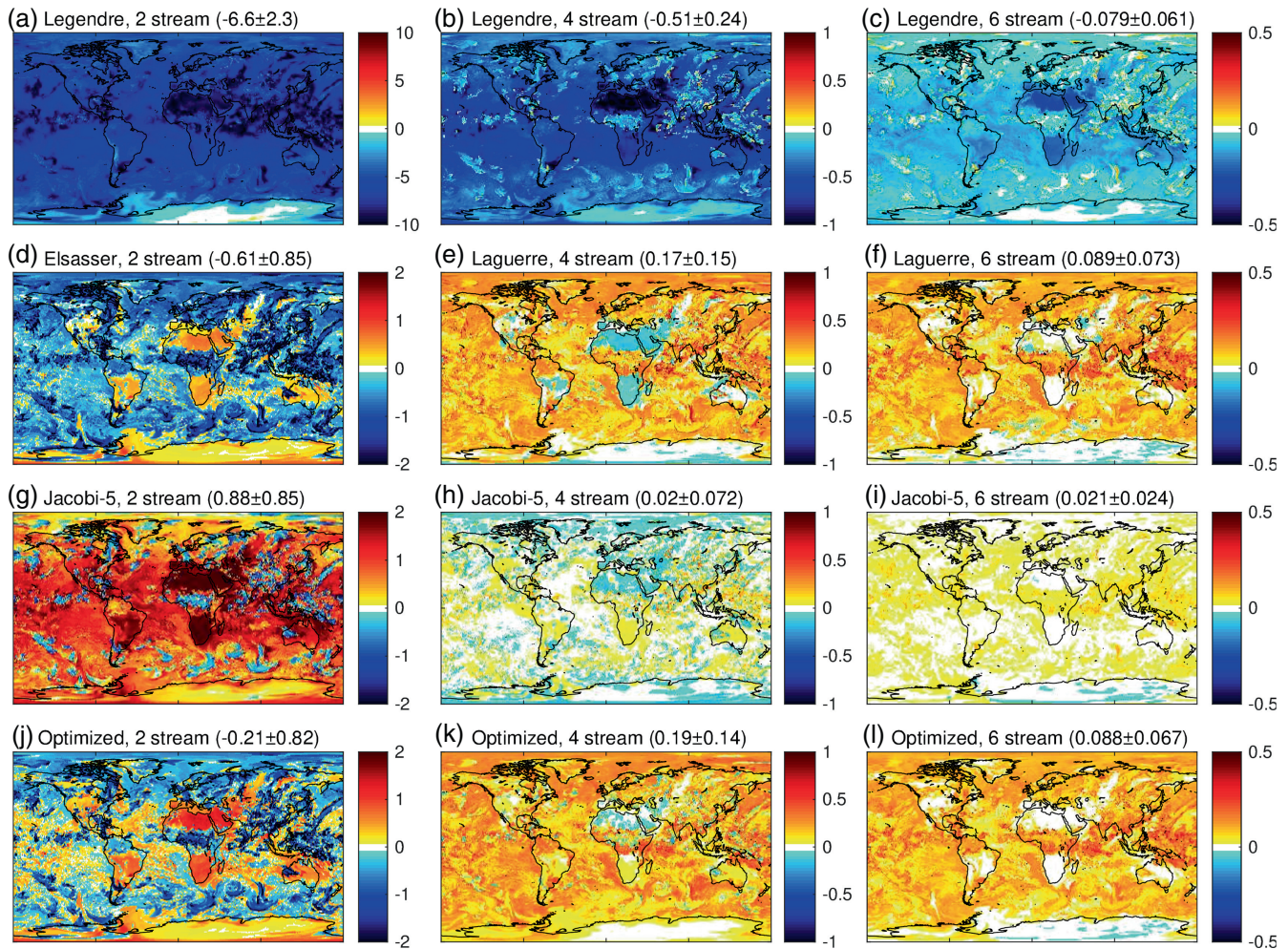


FIGURE 6 Errors in computed top-of-atmosphere upwelling irradiance using ERA5 fields at 1200 UTC on July 11, 2019, for (rows) four different quadrature schemes, using (columns) 2, 4, and 6 streams, in units of $\text{W}\cdot\text{m}^{-2}$. The numbers of the form $B \pm E$ above each panel indicate the global-mean bias (B) and standard deviation of the error (E). Note the different colour scale for each column, and also the much wider colour scale for (a).

instantaneous errors in TOA upwelling and surface downwelling irradiance, respectively, for the ERA5 scene considered in this section. The quadrature schemes shown are Gauss–Legendre, Gauss–Laguerre, Gauss–Jacobi-5, and optimized for 2–6 streams, except that Elsasser’s $D = 1.66$ scheme has been used in place of Gauss–Laguerre for the two-stream case because it is far more widely used and is actually very similar to Gauss–Laguerre (which uses $D = 1.6487$). In the two-stream case, Gauss–Legendre ($D = 2$) performs very poorly, with irradiance biases of around $6 \text{ W}\cdot\text{m}^{-2}$. The other three are much better; optimized quadrature ($D = 1.6402$) is a little better than Elsasser, although the errors in different parts of the world tend to be larger than the global-mean bias. The most striking contrast in these figures is between cloud-free subtropical Africa and the rest of the world. The cloud-free regions are represented particularly poorly by Gauss–Legendre quadrature, but these tend to be the most

accurate regions for the other quadrature schemes in the six-stream case.

The bias (B) and error standard deviation (E) are shown above each panel of Figures 6 and 7. To put these values in perspective, when longwave scattering is turned off in the standard ECMWF longwave scheme for this scene, at TOA we have $B = 1.3 \text{ W}\cdot\text{m}^{-2}$, very similar to the value reported by Hogan and Bozzo (2016), and $E = 1.0 \text{ W}\cdot\text{m}^{-2}$, while at the surface we have $B = -0.4$ and $E = 0.3 \text{ W}\cdot\text{m}^{-2}$. These values are of similar magnitude to the two-stream errors for $D = 1.66$ shown above Figures 6d and 7d. Many climate models still neglect longwave scattering, so these results suggest that there would be little point in increasing the number of streams without also turning on longwave scattering. Note that Lacis and Oinas (1991) used a six-stream scheme yet neglected longwave scattering.

Figure 8 depicts the dependence of clear-sky TOA upwelling and surface downwelling irradiances on column

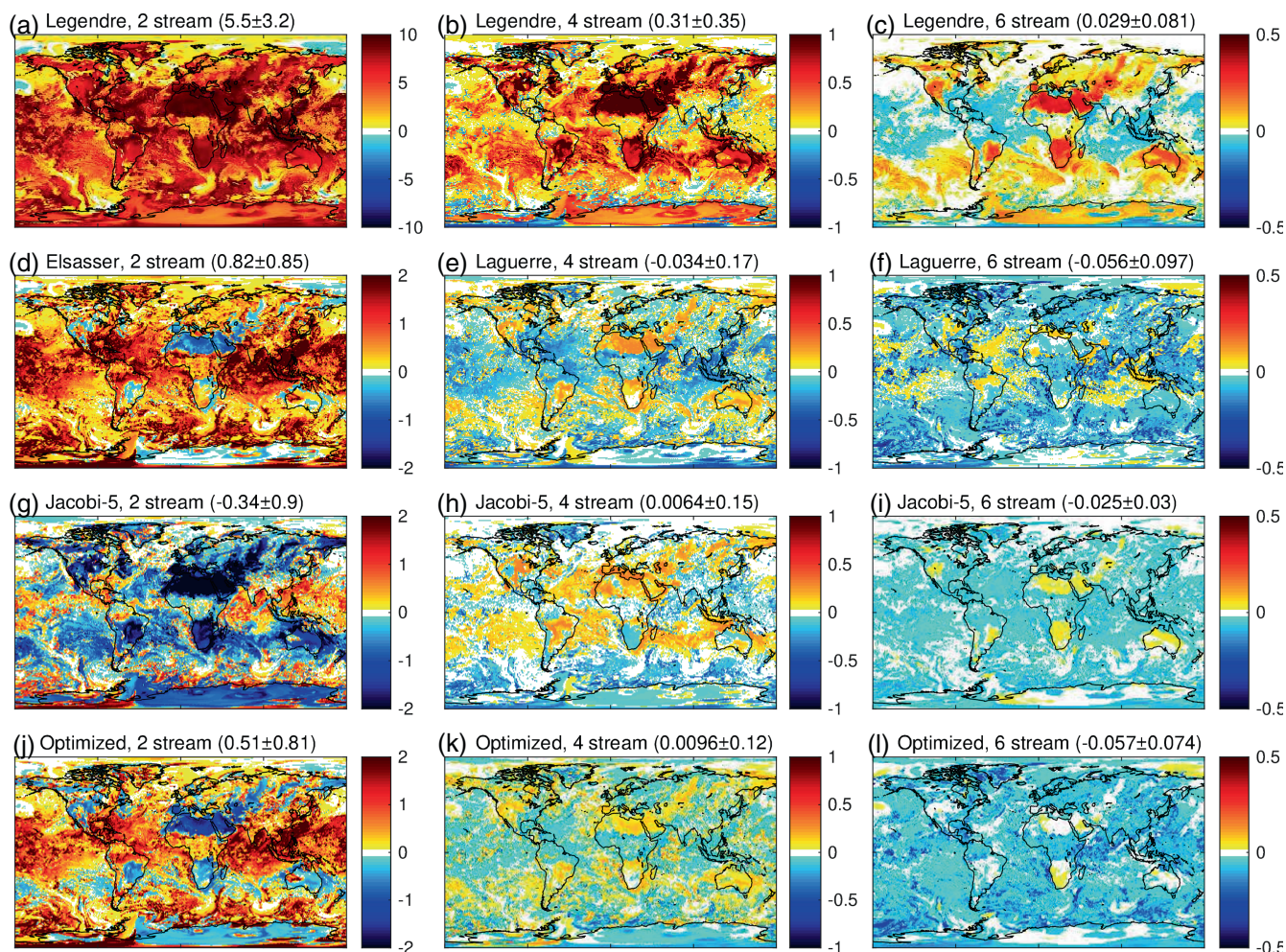


FIGURE 7 As Figure 6 but for surface downwelling irradiance.

water vapour for the same quadrature schemes. While it is again clear that Gauss–Legendre quadrature performs worst up to six streams, the surface irradiance errors of all schemes have a dependence on water vapour that could be important for estimating the impact of changed water vapour on surface temperature. For example, Figure 8d suggests that, as water vapour is increased above $20 \text{ kg}\cdot\text{m}^{-2}$, Elsasser’s scheme predicts that the rate at which surface downwelling irradiance increases will be too large by around $0.1 \text{ W}\cdot\text{m}^{-2} (\text{kg}\cdot\text{m}^{-2})^{-1}$. Figure 8e shows that this is reduced to around $-0.01 \text{ W}\cdot\text{m}^{-2} (\text{kg}\cdot\text{m}^{-2})^{-1}$ for the Gauss–Jacobi-5 and optimized quadratures in the four-stream case.

6 | CONCLUSIONS

The two-stream equations have been the mainstay of atmospheric radiative transfer for many decades but, with ever more resources being found to increase model resolution (e.g. Satoh et al. 2019), now is the time to investigate the

potential benefits of increasing the number of streams in weather and climate models. The radiative transfer problem involves two integrals over the cosine of zenith angle, μ , but the integral to obtain irradiances from radiances is weighted by μ , whereas the integral representing scattering from one stream to another is not. This means that no single set of μ values and corresponding weights (i.e., the quadrature scheme) is optimal for both integrals; in fact, the best-performing scheme depends on how much scattering is present.

By far the most widely used quadrature scheme, and indeed the only one available in DISORT, is Gauss–Legendre applied separately in each hemisphere (also known as “double-Gauss”; Sykes 1951); this is optimal for the scattering integral and so is well suited for shortwave problems. In this article the accuracy and convergence rate of longwave radiative transfer calculations have been rigorously evaluated for a range of quadrature schemes and numbers of streams, making use of our modified version of DISORT that supports alternative quadratures. Because of the much weaker scattering in

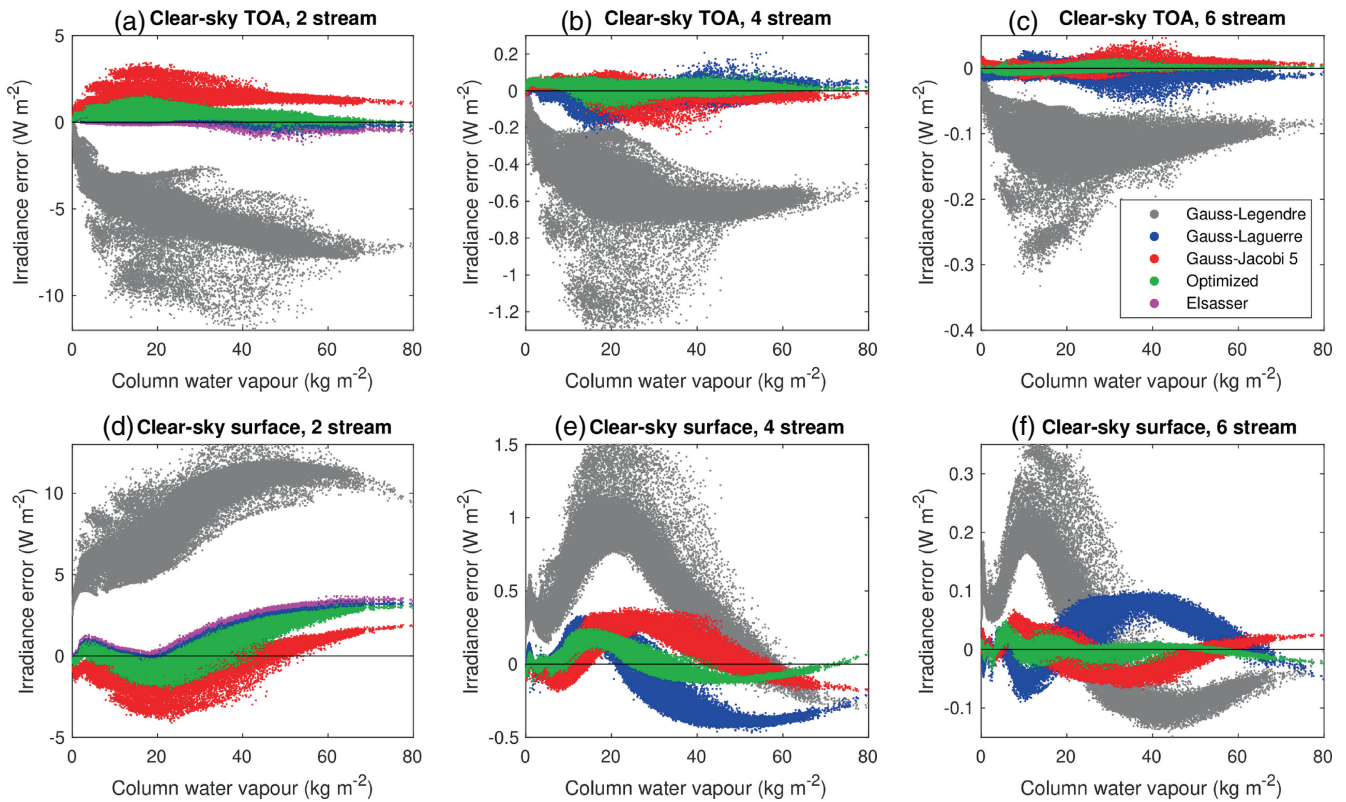


FIGURE 8 Errors in clear-sky (top row) top-of-atmosphere upwelling irradiance and (bottom row) surface downwelling irradiance for the ERA5 scene, as a function of column water vapour, for different quadrature schemes with 2, 4, and 6 streams.

the longwave, we find that Gauss–Legendre is the *least* accurate of all quadratures tested for two- and four-stream radiative transfer. In addition to testing several Gaussian quadrature schemes, we have developed three “optimized” schemes, whereby the angles and weights are chosen to minimize the irradiance and heating-rate errors in a set of clear-sky training profiles. The results are summarized as follows.

- In the two-stream case, the Elsasser (1942) diffusivity of $D = 1.66$ (corresponding to a zenith angle of $\theta_1 = 52.96^\circ$) is close to optimal, although the “optimized” value in this article of $D = 1.6402$ ($\theta_1 = 52.43^\circ$) is a little better for all-sky irradiances, reducing RMSE by around 20% and the magnitude of global-mean biases by 0.3–0.4 $\text{W}\cdot\text{m}^{-2}$. By contrast, the Gauss–Legendre value of $D = 2$ ($\theta_1 = 60^\circ$) leads to an RMSE six times larger.
- The Elsasser and optimized two-stream schemes incur a stratospheric/mesospheric heating-rate bias of 0.25–0.3 $\text{K}\cdot\text{d}^{-1}$, peaking at the stratopause. This is half the magnitude and of the opposite sign to the bias resulting from $D = 2$. Unfortunately, selecting a D to minimize the upper-atmosphere heating-rate bias

would introduce a significant bias in irradiances, a limitation of the two-stream approach.

- For clear-sky calculations in which scattering can be neglected, optimized quadrature out-performs all others examined in this article for any number of streams, and is between one and two orders of magnitude more accurate than Gauss–Legendre. “Gauss–Jacobi-5” quadrature comes a close second.
- For all-sky calculations with 4–8 streams, Gauss–Jacobi-5 quadrature performs best and is recommended for a weather or climate model looking to increase the number of streams it uses to more than two. For 10 or more streams, Gauss–Legendre quadrature is most accurate, except in the stratosphere and mesosphere.
- Following the idea of Lacis and Oinas (1991), we have proposed quadrature schemes for 4–8 streams that are more efficient via the use of μ values that are integer multiples of each other, reducing the number of exponentials that need to be computed. Thus, “optimized-IR” is a more efficient but slightly less accurate version of “optimized” quadrature and “optimized-IRJP” is the same but for Gauss–Jacobi-5.
- We have demonstrated empirically that the quadrature scheme advocated by Li (2000) and which he referred to

as Gaussian quadrature with a moment power of infinity (Gauss–Jacobi– ∞ in our nomenclature) produces identical angles and weights to Gauss–Laguerre quadrature, although in terms of accuracy this is generally inferior to Gauss–Jacobi-5.

The next step will be to implement some of the quadrature schemes proposed here in an atmospheric model and test the impact on weather forecasts and model climate. Two optimizations will be particularly valuable: first, the method of Fu et al. (1997), in which a fast two-stream calculation is used to get an initial estimate of the irradiance profile, followed by the projection of N radiances through the atmosphere using the two-stream fluxes as the scattering source function, yielding more accurate irradiances. Second, the number of exponential calculations can be reduced via use of the optimized-IR and optimized-IRJP quadrature schemes, the μ values of which are integer multiples of each other. Preliminary simulations with the ECMWF model suggest that improved longwave quadrature reduces mean stratospheric temperatures by up to 2 K, as well as changing temperature patterns in the troposphere.

This article has also presented evidence that two-stream schemes may not capture the dependence of surface fluxes on column water vapour correctly, but the magnitude of the effect is reduced by around a factor of 10 when moving to four streams. Further simulations would be required to determine the impact on estimates of the water-vapour feedback.

ACKNOWLEDGEMENTS

I thank Ján Mašek for useful discussions, and Jiangnan Li and the anonymous reviewers for their constructive comments.

CONFLICT OF INTEREST STATEMENT

The author has no conflict of interest to declare.

ORCID

Robin J. Hogan  <https://orcid.org/0000-0002-3180-5157>

REFERENCES

- Abramowicz, M. & Stegun, I. (1972) *Handbook of mathematical functions. 10th printing with corrections*. Washington D.C.: National Bureau of Standards Applied Mathematics Series 55. U.S. Government Printing Office.
- Baum, B.A., Yang, P., Heymsfield, A.J., Bansemer, A., Merrelli, A., Schmitt, C. et al. (2014) Ice cloud bulk single-scattering property models with the full phase matrix at wavelengths from 0.2 to 100 μm . *Journal of Quantitative Spectroscopy & Radiative Transfer*, 146, 123–139.
- Chandrasekhar, S. (1960) *Radiative transfer*. New York: Dover.
- Clough, S.A., Iacono, M.J. & Moncet, J.-L. (1992) Line-by-line calculations of atmospheric fluxes and cooling rates: application to water vapor. *Journal of Geophysical Research*, 97, 15761–15785.
- DeSouza-Machado, S., Strow, L.L., Motteler, H. & Hannon, S. (2020) kCARTA: a fast pseudo line-by-line radiative transfer algorithm with analytic Jacobians, fluxes, nonlocal thermodynamic equilibrium, and scattering for the infrared. *Atmospheric Measurement Techniques*, 13, 323–339.
- Elsasser, W.M. (1942) *Heat transfer by infrared radiation in the atmosphere*, Harvard meteorological studies, 6. Milton, MA: Harvard University Press.
- Feng, J. & Huang, Y. (2019) Diffusivity-factor approximation for spectral outgoing longwave radiation. *Journal of the Atmospheric Sciences*, 76, 2171–2180.
- Fu, Q., Liou, K.-N., Cribb, M.C., Charlock, T.P. & Grossman, A. (1997) Multiple scattering parameterization in thermal infrared radiative transfer. *Journal of the Atmospheric Sciences*, 54, 2799–2812.
- Hogan, R.J. (2010) The full-spectrum correlated- k method for longwave atmospheric radiation using an effective Planck function. *Journal of the Atmospheric Sciences*, 67, 2086–2100.
- Hogan, R.J. (2014) Fast reverse-mode automatic differentiation using expression templates in C++. *ACM Transactions on Mathematical Software*, 40, 26:1–26:16.
- Hogan, R.J. (2019) Flexible treatment of radiative transfer in complex urban canopies for use in weather and climate models. *Boundary-Layer Meteorology*, 173, 53–78.
- Hogan, R.J. & Bozzo, A. (2016) *ECRAD: a new radiation scheme for the IFS*. Reading, UK: ECMWF Tech. Memo, No. 787.
- Hogan, R.J. & Bozzo, A. (2018) A flexible and efficient radiation scheme for the ECMWF model. *Journal of Advances in Modeling Earth Systems*, 10, 1990–2008.
- Hogan, R.J. & Matricardi, M. (2020) Evaluating and improving the treatment of gases in radiation schemes: the correlated K -distribution model Intercomparison project (CKDMIP). *Geoscientific Model Development*, 13, 6501–6521.
- Hogan, R.J. & Matricardi, M. (2022) A tool for generating fast k -distribution gas-optics models for weather and climate applications. *Journal of Advances in Modeling Earth Systems*, 14, e2022MS003033.
- Kautsky, J. & Elhay, S. (1982) Calculation of the weights of interpolatory quadratures. *Numerische Mathematik*, 40, 407–422.
- Lacis, A. & Oinas, V. (1991) A description of the correlated k -distribution method for modeling nongray gaseous absorption, thermal emission, and multiple scattering in vertically inhomogeneous atmospheres. *Journal of Geophysical Research*, 96, 9027–9063.
- Li, J. (2000) Gaussian quadrature and its application to infrared radiation. *Journal of the Atmospheric Sciences*, 57, 753–765.
- Liu, D.C. & Nocedal, J. (1989) On the limited memory method for large scale optimization. *Mathematical Programming Series B*, 45, 503–528.
- Meyer, D., Hogan, R.J., Dueben, P.D. & Mason, S.L. (2022) Machine learning emulation of 3D cloud radiative effects. *Journal of Advances in Modeling Earth Systems*, 14, e2021MS002550.
- Mlawer, E.J., Taubman, S.J., Brown, P.D., Iacono, M.J. & Clough, S.A. (1997) Radiative transfer for inhomogeneous atmospheres: RRTM, a validated correlated- k model for the

- longwave. *Journal of Geophysical Research – Atmospheres*, 102, 16663–16682.
- Press, W.H., Teukolsky, S.A., Vetterling, W.T. & Flannery, B.P. (2007) *Numerical recipes: the art of scientific computing*, 3rd edition. Cambridge: Cambridge University Press.
- Rodgers, C.D. & Walshaw, C.D. (1966) The computation of infrared cooling rates in planetary atmospheres. *Quarterly Journal of the Royal Meteorological Society*, 92, 67–92.
- Satoh, M., Stevens, B., Judt, F., Khairoutdinov, M., Lin, S.-J., Putman, W.M. et al. (2019) Global cloud-resolving models. *Current Climate Change Reports*, 5, 172–184.
- Schuster, A. (1905) Radiation through a foggy atmosphere. *The Astrophysical Journal*, 21, 1–22.
- Stamnes, K., Tsay, S.-C., Wiscombe, W. & Jayaweera, K. (1988) Numerically stable algorithm for discrete-ordinate-method radiative transfer in multiple scattering and emitting layered media. *Applied Optics*, 27, 2502–2509.
- Sykes, J.B. (1951) Approximate integration of the equation of transfer. *Monthly Notices of the Royal Astronomical Society*, 111, 377–386.
- Toon, O.B., McKay, C.P., Ackerman, T.P. & Santhanam, K. (1989) Rapid calculation of radiative heating rates and photodissociation rates in inhomogeneous multiple scattering atmospheres. *Journal of Geophysical Research*, 94, 16287–16301.
- Wiscombe, W.J. (1977) The delta-*M* method: rapid yet accurate radiative flux calculations for strongly asymmetric phase functions. *Journal of the Atmospheric Sciences*, 34, 1408–1422.
- Zhao, J.-Q. & Shi, G.-Y. (2013) An accurate approximation to the diffusivity factor. *Infrared Physics & Technology*, 56, 21–24.

How to cite this article: Hogan, R.J. (2023) What are the optimum discrete angles to use in thermal-infrared radiative transfer calculations?. *Quarterly Journal of the Royal Meteorological Society*, 1–16. Available from: <https://doi.org/10.1002/qj.4598>